SIGMA PHASE FORMATION IN A HEAT TREATED NI-50CR COATING APPLIED BY HVOF PROCESS ON A STAINLESS STEEL

J. Saaedi[1, 2], H. Arabi[1], Sh. Mirdamadi[1] and Th. W. Coyle[2]
saaedi@iust.ac.ir

Date of Recieve: July 2008 Date of Acceptance: November 2008

[1] Department of Metallurgy and Materials Engineering, Iran University of Science and Technology, Tehran, Iran

[2] Centre for Advanced Coating Technologies, Department of Materials Science and Engineering, University of Toronto, Toronto, Canada.

Abstract: *Two different coating microstructures of Ni-50Cr alloy were obtained on a stainless steel substrate by changing combustion characteristics of a high velocity oxy-fuel (HVOF) process and the size distribution of feed powder during coating process. Use of the finer feed powder and leaner fuel in oxygen/fuel ratio (i.e. using a ratio much less than stoichiometric ratio) led to formation of an extremely dense coating with high oxide content. Heat treating of this coating at 650ºC for 4 hours caused the formation of an intermetallic sigma phase having Cr_7Ni_3 stoichiometry. Formation of this phase has been reported occasionally in thin films not in thermal spray coatings, as reported for the first time in this research. In addition no sigma phase was detected in the HVOF as-deposited coating with low oxide content after heat treatment of the samples. Therefore, due to the limited number of papers available in the subject of formation of σ phase in either Ni-Cr bulk alloys or coatings, it is considered appropriate to show up a case in this field. In this work, the formation of sigma phase in Ni-50Cr coating deposited by HVOF technique and heat treated at 650ºC was discussed and then the coating was characterized.*

Keywords: *sigma phase; HVOF; oxide phases; thermal sprayed coatings; Ni-50Cr.*

1. INTRODUCTION

Sigma phase is an intermetallic tetragonal closed packed (tcp) phase which has been commonly found in alloys of the transition metals of the first long period and especially described in Fe–Cr alloy system [1]. Sigma phase is said to be formed with a wide range of compositions and various morphologies which may be detrimental to properties. However, the presence of σ in superalloys is not necessarily damaging their properties [2]. Sigma in the form of platelets or as a grain-boundary film is detrimental, but in the form of globular intragranular precipitation can improve creep properties [2].

Considerable efforts have been developed to determine how composition influences σ-phase formation, particularly in nickel-base superalloys [2]. A reliable method for predicting σ-phase formation is based on the theory of electron vacancies of the atoms entering into the σ-phase lattice [3]. Sully and Heal [4] have already suggested a theory based on which sigma occurrence may be determined by a critical electron: atom ratio. Using this ratio, the theory predicts the appearance of sigma-phase in some alloy systems including Ni-Cr system. In some of the binary alloy systems the sigma phase has been shown to occur over a wide range of composition [5]. It is of interest to note that, although the theory predicts the appearance of the sigma-phase in Ni-Cr system having 71.8 at% (69.2 wt%) Cr, but the exact range of Cr content has not been established.

This might be due to the upper temperature limit for stability of the phase which varies from system to system. This temperature for nickel-chromium system is very low, so that transformation does not occur in a reasonable period of time [5].

It has been referred in other studies [6] that in addition to the chemical composition of the alloys, their microstructures have a marked effect on the formation of σ-phase. This has not

considered in the theory of electron vacancies of the atoms. The process of σ-phase formation for different structures is markedly different. For example, the most intense σ-phase formation occurs in cast metal as the result of its high inhomogeneity [6]. As the degree of microstructural homogeneity increases for the metal (i.e. cast → extruded → forged respectively) the process of σ-phase formation slows down, and the temperature range for the existence of σ-phase contracts [6]. Simultaneously there is a reduction in the temperature for precipitation of intense σ-phase in cast structures [6].

In Ni–Cr thin films, the σ-phase was occasionally reported in the literature [7], although σ-phase is not shown on the equilibrium Ni-Cr phase diagram describing bulk alloys. It is said [8] that this phase is thermodynamically more stable than the solid solution phases in thin films over a composition range extending from about 47% Cr to roughly 83% Cr at 25 °C.

Modern thermal spray processes such as high velocity oxy-fuel (HVOF) and plasma spraying are often applied to deposit high-chromium, nickel-chromium coatings onto the surface of various parts to prevent high temperature oxidation and hot corrosion in gas turbines and other equipment [9]. However, the thermal spray coatings exhibit certain drawbacks compared to cast alloys [9].

During thermal spraying the heated and potentially molten, oxidized, or vaporized particles strike the substrate whereupon they deform (i.e. splat) and adhere through predominantly mechanical interlocking (mechanical bonding) mechanisms [10]. The hot particles are exposed to air atmosphere, which results in oxide layers at splat boundaries. In addition, thermal spray coatings may include un-melted particles, residual porosity, and cracks, resulting in an inhomogeneous structure. The microstructure of a thermal sprayed coating is significantly affected and controlled through used process parameters during spraying [6].

HVOF combustion temperatures and characteristics depend on the stoichiometry of the oxygen-fuel mixtures. The ratio of fuel to oxygen is important in determining the final coating structure. Ideal stoichiometric combustion of propylene requires a 4.5:1 ratio of oxygen to fuel molecules ($C_3H_6 + 4.5O_2 = 3H_2O + 3CO_2$). If the combustion ratio is lean in fuel, unconsumed oxygen molecules in the flame create an "oxidizing" environment. This condition results in excessive oxidation of the molten metallic powder particles, thus leading to a high level of oxides in the coating. A fuel-rich mixture creates an oxygen-depleted "reducing" flame of low temperature, resulting in an increase in unmelted particles and porosity having low oxide content [11].

On the other hand, cooling rate of HVOF as-deposited coatings is very high, typically in excess of 10^6 K/s for metals [12], so that non-equilibrium, metastable, crystalline and amorphous phases can be formed which are not usually expected to be formed in equilibrium phase diagrams. The phases formed after coating deposition, transform to more stable structures when expose to the high temperatures service. An understanding of the process variables and the resulting structures formed after deposition of coating as well as in high temperature service can provide new insights into coatings technology.

2. EXPERIMENTAL WORKS

Two commercial Ni-50Cr Powders were deposited onto 310 stainless steel (25Cr-20Ni) plates by different HVOF process parameters

Table. 1. Sizes and compositions of the powders.

No.	Powder	Composition (wt %)						Nominal Size (μm)
		C	Cr	Fe	Mn	Si	Ni	
1	Sulzer Metco AMDRY 350F	0.03	49.6	0.1	0.1	0.3	Bal.	-44
2	Praxair TAFA 1260F	0.041	46	1.2	0.003	0.8	Bal.	+20/ -53

Table. 2. Process parameter settings used for deposition of the powders

Parameter / Powder No.	Oxygen Flow (SLM)	Propylene Flow (SLM)	Air Flow (SLM)	Oxygen/Fuel ratio	Stand-off Distance (mm)	Feed Rate (g/min)
1	303	87	354	3.5	230	23
2	136	96	354	1.4	230	61

using a Sulzer Metco DJ 2700 Gun (see Tables 1 and 2). The thicknesses of the coatings were approximately 200 ±20 μm.

Coated substrates were sectioned and polished for microstructural characterization using optical microscopy (OM) and scanning electron microscopy (SEM). The scanning electron microscopes used in this work was a JEOL JSM-840 (SEM) attached to a PGT/AAT EDS detector (thin window).

The phase compositions of the powder and coatings were characterized by X-ray diffraction (XRD) using a Philips PW 2273/20 diffractometer with Cu Kα radiation and a scanning rate of 1.45 degrees/min. The diffractometer was operated at 40 kV and 40 mA. The XRD analyses were conducted on a lightly compacted powder sample, the top of as-deposited and heat treated surfaces of the coatings.

The coated samples were heat treated at 650 ºC for 1 and 4 hours under vacuum in a Red Devil high temperature vacuum furnace. Heating rate was 10ºC/min and the samples were cooled in the furnace to the room temperature.

3. RESULTS AND DISCUSSION

Both oxygen/fuel ratios used to deposit the powders 1 and 2 were fuel-rich compared to the stoichiometry ratio. However this ratio for deposition of powder 2 was quite far from the stoichiometry ratio (i.e. 0.3 of the stoichiometry ratio) and much rich in fuel. Typical profiles of the coated samples for powders Nos. 1 and 2 are shown in Figs. 1 and 2.

The microstructure of coating 1 includes light Ni-Cr matrix with a high amount of dark oxides between the splats. This coating was much dense with a low amount of pores. The splats in this coating are remarkably flat and have wavy shape, Fig. 1. The microstructure of coating 2 includes of very low oxide content with more pores (black areas in Fig. 2). Moreover the splats are not flat and a great number of them are in un-melted and semi-melted conditions.

The oxide content observed within the coating microstructures (see Figs. 3 & 4) was due to oxidation during coating process as this has been confirmed by other researchers [13]. Oxidation in thermal spraying can occur in three stages according to Korpiola [13]; 1. Particles are mainly oxidized in the combustion chamber and acceleration tube of the thermal spray gun by the oxidizing combustion products (i.e. CO^2, H^2O and free oxygen atoms) present at high temperatures. Recent work by Korpiola [14] has showed that about 70% of the oxidation of the HVOF NiCr80/20 coatings occurred in this stage; 2. Oxidation takes place during the flight by

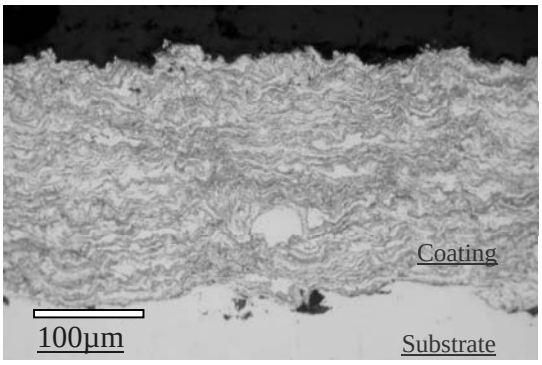

Fig. 1. OM image of As-deposited Coating 1

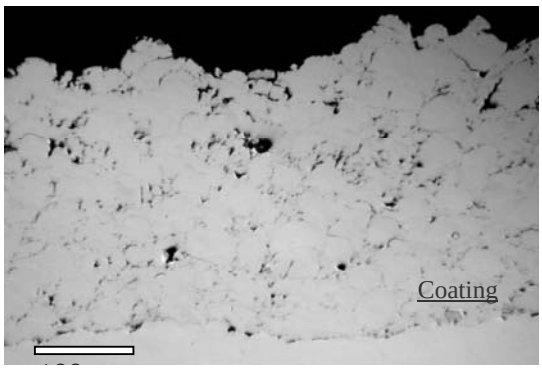

Fig. 2. OM image of As-deposited Coating 2

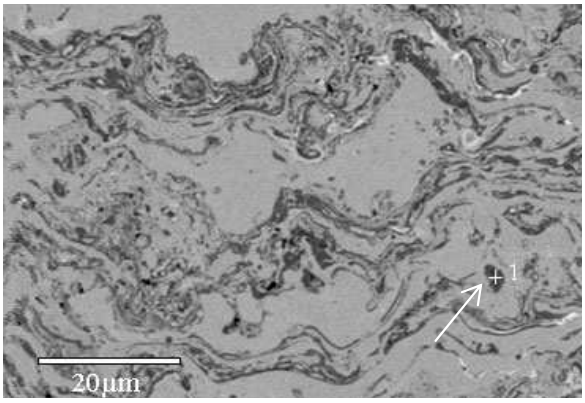

Fig. 3. BSE image of as-deposited Coating 1

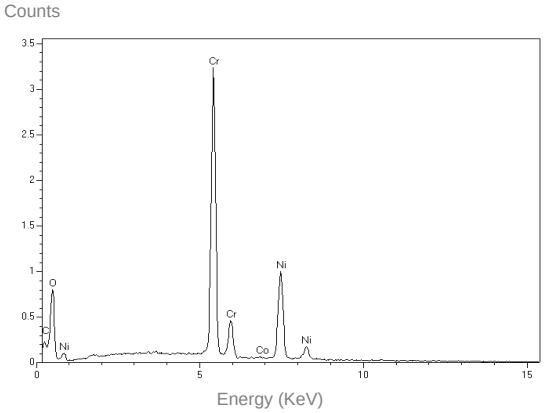

Fig.4. EDS spot analysis on Point 1 of Fig. 3

oxygen entrained into the mixing plume from the surrounding air; 3. Oxidation of splats takes place on the substrate during solidification.

In HVOF the oxidation capacity which is the amount of oxygen in the flame available for oxidation of a given material, is related to the ratio of oxidizing and reducing gaseous species. Oxygen potential indicates the ability of the flame to oxidize metals or compounds in spray powder mixture. A metal powder is in principle able to pick up oxygen from the oxidizing gaseous species of the hydrocarbon combustion flame for oxide formation down to the level corresponding to the equilibrium of oxidation reaction of an element, for example, chromium [13].

The above discussion indicates that fuel/oxygen ratio could be considered to play a very important role in oxidation of thermal spraying. The effect of this ratio on oxidation was clearly observed in this work by comparing the microstructures of two coatings which deposited by means of two different fuel/oxygen ratios. However due to high Cr content of the alloy (i.e. ~50 wt%) which makes it very susceptible to oxidation, one needs to use much fuel/oxygen ratios than that of the stoichiometric ratio if he/she designs to obtain coatings with low oxide content for HVOF deposition of Ni-50Cr powder.

Typical energy dispersive x-ray spectroscopy (EDS) analyses of the dark areas (shown in Figs. 1 & 3) in as-polished cross section of coating 1 confirmed that these areas were mostly nickel-chromium oxides. However it was not possible to determine the composition the oxide phases due to the very fine scale features within these dark areas and the limited spatial resolution of EDS available. More discussion about the characteristics of these oxide phases has been presented elsewhere [15].

XRD patterns of powders 1 and 2 show that the powders were single phase, as no secondary phases were detected, see Fig. 5. The patterns exhibit three peaks which were assigned to the (111), (200) and (220) planes of γ-Ni, however one should notice that these peaks were slightly shifted to the left relative to pure nickel peaks, due to the present of Cr in the form of solid solution in the alloy.

For the as-deposited coatings 1 and 2, approximately similar pattern to those of powders 1 and 2 were obtained, Fig. 6. Broadening of peaks in Fig. 6 was interpreted as the differences in compositions of γ -Ni phase within the splats. This indicates that the total composition of the γ-Ni phase in the coating did not changed such that a new phase could be formed.

In the case of coating 1, minor differences in the form of several small new peaks were observed in the XRD patterns in comparison to that of powder 1. The shoulders appeared in the γ-Ni peaks of Fig. 6 may be due to the presence of a second γ-Ni phase with lower chromium content and/or due to the same γ-Ni with different composition. Two additional small, broad peaks were seen in the XRD patterns of the coating 1 (see Fig. 6) and located near the positions of major peaks of nickel-chromium oxide ($NiCr_2O_4$) seemed to be related to $NiCr_2O_4$ as these type of peaks have been also reported in reference [17]. More experimental works indicated that the most of the oxides formed after

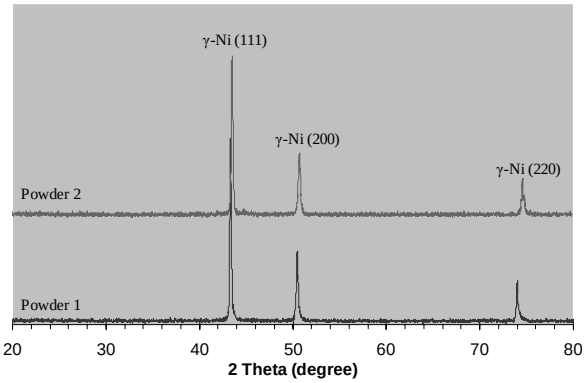

Fig.5. XRD patterns of Powders 1 and 2 in comparison to the reference patterns of Ni [16].

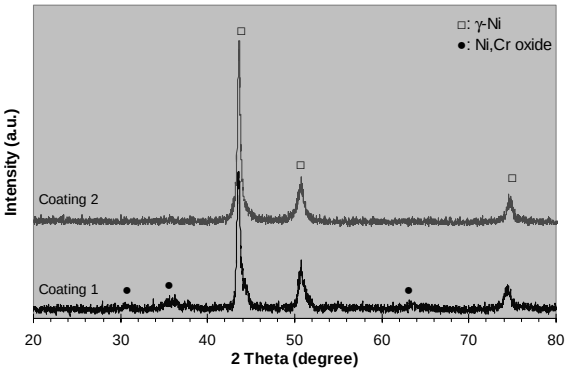

Fig. 6. XRD patterns of Coatings 1 and 2

deposition of this kind of coatings are poorly crystallized or exist as very thin layers or small particles which are not detectable by XRD [15].

Simultaneously heat treating of both coatings at 650°C led to formation of an intermetallic sigma tcp phase in coating 1 (Fig. 7). The detected sigma phase had composition near to Cr_7Ni_3 as reported in a few articles [18-20].

Table 3 has shown X-ray diffraction data reported for the sigma phase in the literature, as well as the data obtained in this research. The data obtained in the present study are in a good agreement with those of Naohara et al. [18] which also referred by International Center for Diffraction Data (ICDD) [19].

In addition to sigma phase the XRD patterns, Fig. 7, of heat treated samples exhibited sharp other peaks which were assigned to three different phases: fcc γ-Ni, bcc α Cr, and Cr_2O_3. The Cr_2O_3 peaks were only observed in coating 2. According to Ni-Cr phase diagram (Fig. 8), a two-phase mixture of fcc γ-Ni with 33 wt% Cr and bcc α-Cr with 2-3 wt% Ni are in equilibrium at 650°C. Therefore decomposition of supersaturated γ-Ni of the as-deposited coatings after heat treatment into the fcc γ-Ni with lower chromium content and bcc α Cr are in consistent with Ni-Cr phase diagram. No detectable oxide was observed in XRD pattern of Coating 2 which simultaneously heat treated with Coating 1. Hence it could be concluded that the formation of Cr_2O_3 in coating 1 was from weakly diffracting non-equilibrium oxide phases, shown in Fig. 6, amorphous or poorly crystallized mixed oxides, and oxygen trapped in splat boundaries or other pores in the as-deposited coatings [15].

Many efforts were done in this research to reveal the sigma phase in the microstructure of heat treated coating 1 by means of the different etchants which could be expected to etch preferably sigma phase. Aqua regia [22], Modified Murakami [23], and Marbel reagent [6] utilized in order to reveal the sigma phase in the microstructure. However positive identification by etching was not obtained. This may be due to the wide range of alloy compositions in chromium-rich phases and fine scale features in HVOF microstructure of this alloy. Nevertheless a comparison between XRD patterns of coatings 1 and 2 indicated that the σ formation in coating 1 occurred in association with the oxide phases which had relatively large sizes. No sigma phase observed in the XRD pattern of coating 2 after the heat treatment even though the as-deposited coating had low quantity of oxides with small size and non-continuous oxide film on splats boundaries.

The σ formation in nickel-base superalloys is said to be related to destabilization of the fcc matrix which is connected to segregation of an intermetallic hardening γ'-phase, within which the solubility of chromium, molybdenum, and cobalt is low, and consequently, the precipitation of σ from the new fcc matrix rich in the above mentioned elements can occur [24, 25]. In this study it could not be presumed that sigma phase formed in connection with decomposition of supersaturated γ-Ni and precipitation of γ-Cr in interior of the splats as transformation of supersaturated γ-Ni phase occurred in case of Coating 2 without formation of sigma phase. Therefore sigma phase formed in Coating 1 after the heat treatment should be connected to the

Table. 3. XRD data for Cr-Ni sigma phase

			Yukawa [20]		Naohara [18]		ICDD [19]		Present study	
h	k	l	d(Å)	I	d(Å)	I	d(Å)	Int-f	d(Å)	I/I_0
4	1	0	2.111	vvw	2.108	s	2.108	100m	2.108	100
1	1	2			2.108	s		m		
3	3	0	2.068	m	2.040	vw		5		
2	0	2	2.033	vs	1.998	m	1.998	50	1.998	48
4	1	1	1.932	vvw	1.907	w	1.907	10	1.907	22
3	3	1	1.888	vvw	1.873	vw	1.873	5	1.877	19

existence of presumably large size oxide phases.

Ogawa and Omura [26] observed the nucleation of Fe-Cr sigma phase in low temperature heat affected (700-1000ºC) zone of a duplex stainless steel after heating during welding. They concluded that since the form of an austenite phase does not change in this temperature range of a low temperature HAZ, the formation of sigma phase nuclei is greatly affected by the presence of oxide inclusions in the parent metal. That is, since the free energy at the interface of inclusions and a steel matrix is high, nuclei having a reduced energy due to precipitation can be formed easily. They found that interface of coarse inclusions having above a certain size (i.e. >5 micrometers) are harmful inclusions as they can promote sigma phase precipitation, and therefore reducing their density is effective at suppressing precipitation of sigma phases in a HAZ.

Naohara and Shinohara [18] identified the accelerated formation of the sigma phase on the surface of cast sample of the alloy of 70 at% Cr-30 at% Ni which aged at 700°C for 165 hours in air. They proposed that the sigma phase was transformed not from the γ-Ni phase but from the α-Cr phase favorably at the interface between Cr_2O_3 and the α-Cr phase. The formation of sigma phase in this work seems to be partially in a same manner. In other words, the sigma phase seemed to be initiated in vicinity of large oxide phase having high surface energy. XRD data reported by the International Center for Diffraction Data (ICDD) reference pattern [21] for sigma phase are in good agreement with the results obtained in this research for sigma phase formed in coating 1. Moreover the ICDD report noted that the ó phase appears along with Cr_2O_3. In co-evaporated 50-75% Cr thin films [8] which was annealed at temperatures above 300 °C sigma phase formation has been reported to be along with the formation of one or both terminal solid solution phases in combination with an oxide microconstituent such as α-Cr_20_3 or $NiCr_20_3$. These results confirm the σ formation in combination with oxide phases in the HVOF coatings.

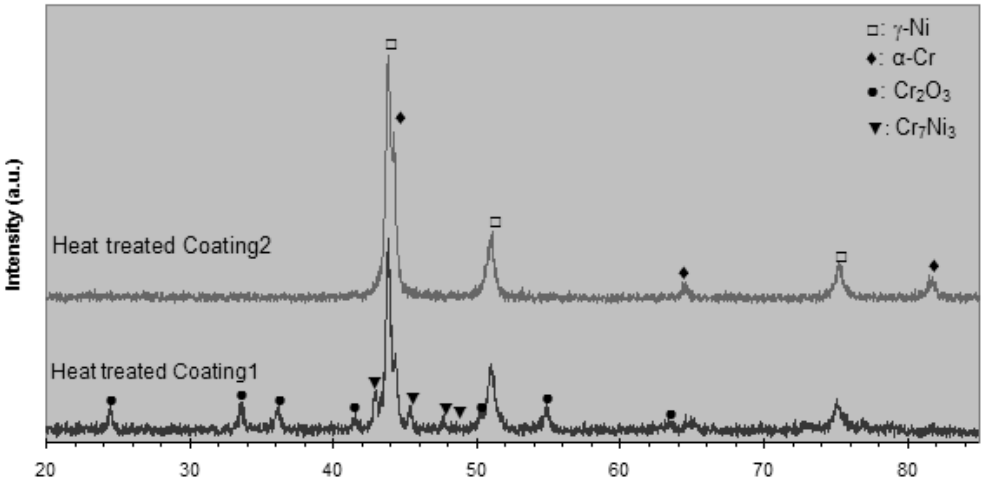

Fig.7. XRD patterns of Coatings 1 after heat treatment at 650ºC

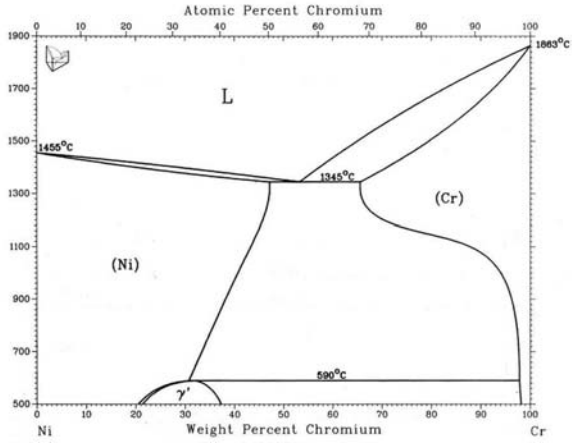

Fig. 8. Nickel-Chromium phase diagram [21]

REFERENCES

1. The Ni-50Cr alloy was easily oxidized in a great extent after HVOF spraying even by means of the fuel-rich flames.

2. Using the feed powder with coarser particle size distribution and also the oxygen/fuel ratio of quite far (about 0.3 time) from the stoichiometry ratio in HVOF spraying led to formation of a coating with low oxide content.

3. A sigma phase with composition of 70 at% Cr and 30 at% Ni was detected by XRD analysis on the HVOF as-deposited coating which heat treatment at 650ºC for 4 hours. Identification of this phase was not possible by application of different etchants possibly due to the wide range of alloy compositions in chromium-rich phases and fine scale features in HVOF microstructure of this alloy.

4. The sigma formation in this coating seemed to be associated with the existence of coarse oxide phases in the microstructure of as-deposited coating. This phase was likely initiated from the interface of α-Cr phase with oxide phase and its formation was confined to extremely thin layers.

ACKNOWLEDGMENT

Thanks are expressed to Dr. Larry Pershin and Tiegang Li for help with deposition of the coatings. Partial support for J. Saaedi during the course of this work was provided by the Centre for Advanced Coating Technologies, University of Toronto, Toronto, Canada, Professor Javad Mostaghimi, Director.

REFERENCES

1. N. Yukawa, M. Hida, T. Imura, M. Kawamura, and Y. Mizuno, Structure of chromium-rich Cr-Ni, Cr-Fe, Cr-Co, and Cr-Ni-Fe alloy particles made by evaporation in argon, Metallurgical Transactions, Vol. 3, 1972, 887.

2. J. R. Davis (Ed.), ASM Specialty Handbook, nickel, cobalt, and their alloys, ASM International, 2000, p. 304.

3. V.B. Kireev, N.V. Kolyasnikova and V.V. Matyushenko, Effects of composition on the formation of the sigma-phase in nickel alloys, Metal science and heat treatment, Vol. 31, No. 12, 1989.

4. A. H. Sully, The Sigma Phase in Binary Alloys of the Transition Elements, Journal of the Institute of Metals, Vol. 80, 173 (1951–52).

5. A. H. Sully, Sigma-Phase in Transitional Metal Alloys, Nature 167, March 1951, 365 – 366.

6. L. S. Bulavina and I. N. Melkumov, Formation of sigma-phase in alloy KhN65VMTYu, Metal science and heat treatment, Vol. 29, No. 4, 1987.

7. W. Brückner, W. Pitschke, and J. Thomas, Stress, resistance, and phase transitions in NiCr 60 wt% thin films, J. Applied Physics, Vol. 87, No. 5, 2000.

8. M. B. Vollaro and D. I. Potter, Phase formation in coevaporated Ni-Cr thin films, Thin Solid Films, 239 (1994) 37-46.

9. J. Tuominen, P. Vuoristo, T. Mäntylä, S. Ahmaniemi, J. Vihinen, and P.H. Andersson, Corrosion behavior of HVOF-sprayed and Nd-YAG laser-remelted high-chromium, nickel-chromium coatings,

Journal of Thermal Spray Technology, Vol. 11(2) June 2002, 233.

10. K. Luer, J. Du Pent, and A. Marder, High Temperature Sulfidation of Fe3Al and NiCr Thermal Spray Coatings at 600°C, CORROSION/1999 NACE, Houston 2001, Paper No. 298.

11. D. J. Varacalle, M. G. Ortiz, C.S. Miller, A.J. Rotolico, J. Nerz, T.J. Steeper, and W.L. Riggs, HVOF combustion spraying of inconel powder, Proc. International Thermal Spray Conference & Exposition, Orlando, 1992, USA, p 181.
12. J.R. Davis (Ed.), Handbook of Thermal Spray Technology, ASM International, 2004, p. 3

13. K. Korpiola, H. Jalkanen, H. Jalkanen, L. Laas, and F. Rossi, Oxygen partial pressure measurement in the HVOF gun tail flame, Proceedings of the 8th National Thermal Spray Conference, 11-15 Sep. 1995, Houston, USA, p. 181.

14. K. Korpiola, High temperature oxidation of metal, alloy and cermet powders in HVOF spraying process, Doctoral Thesis, Helsinki University of Technology, 2004, p. 81.

15. J.Saaedi, T. W. Coyle, S. Mirdamadi, H. Arabi, and J. Mostaghimi, Phase formation in a Ni-50Cr HVOF coating, Surface and Coating Technology, in Press.

16. JCPDS, International Centre for Diffraction Data, 2005, PDF # 00-004-0850.

17. JCPDS, International Centre for Diffraction Data, 2005, PDF # 01-075-1728.

18. T. Naohara and K. Shinohara, Sigma phase formation in Cr-Ni binary alloy system, Scripta Metallurgica, Vol. 17, 1983, 111-114

19. JCPDS, International Centre for Diffraction Data, 2005, PDF # 00-051-0637.

20. N. Yukawa, M. Hida, T. Imura, M. Kawamura, and Y. Mizuno, Structure of chromium-rich Cr-Ni, Cr-Fe, Cr-Co, and Cr-Ni-Fe alloy particles made by evaporated in argon, Metall. Trans. 3, 1972, 887.
21. Th. B. Massalski, Binary Alloy Phase Diagrams, ASM International, 1986, Vol. 1, p. 842.

22. G. F. Vander Voort, Metallography, Principles and Practice, McGraw-Hill, 1984, p 649.

23. R. L. Dreshjeld and R. L. Ashbrook, Further observations on the formation of sigma phase in a nickel-base superalloy (IN-100), NASA Technical Note D-6015, National Aeronautics and Space Adminstration, USA, 1970.

24. G.D. Pigrova, TCP-phases in nickel-base alloys with elevated chromium content, Metal Science and Heat Treatment Vol. 47, Nos. 11 – 12, 2005.

25. A. K. Jena and M. C. Chaturvedi, Review the role of alloying elements in the design of nickel-base superalloys, Journal of Materials Science 19 (1984) 3121-3139.

26. K. Ogawa and T. Omura, Duplex stainless steel, US Patent 20060191605, 2006.